Penerbit Akademia Baru

Journal of Advanced Research in Fluid Mechanics and Thermal Sciences

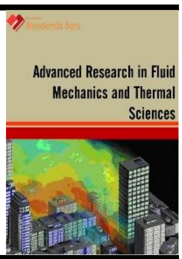

Journal homepage: www.akademiabaru.com/arfmts.html
ISSN: 2289-7879

Numerical Investigation of Heat Transfer Enhancement with Ag-GO Water and Kerosene Oil Based Micropolar Nanofluid over a Solid Sphere

Open Access

Mohammed Z. Swalmeh[1,2], Hamzeh T. Alkasasbeh[3], Abid Hussanan[4,5 *], Mustafa Mamat[1]

[1] Faculty of Informatics and Computing, Universiti Sultan Zainal Abidin (Kampus Gong Badak), 21300 Kuala Terengganu, Terengganu, Malaysia
[2] Faculty of Arts and Sciences, Aqaba University of Technology, Aqaba, Jordan
[3] Department of Mathematics, Faculty of Science, Ajloun National University, P.O. Box 43, Ajloun 26810, Jordan
[4] Division of Computational Mathematics and Engineering, Institute for Computational Science, Ton Duc Thang University, Ho Chi Minh City, Vietnam
[5] Faculty of Mathematics and Statistics, Ton Duc Thang University, Ho Chi Minh City, Vietnam

ARTICLE INFO

Article history:
Received 24 March 2019
Received in revised form 15 May 2019
Accepted 25 June 2019
Available online 20 July 2019

Keywords:
Micropolar nanofluid; Mixed convection; Solid sphere; Keller box method

ABSTRACT

In this paper, the micro-rotation and micro-inertia characteristics of nanofluids under mixed convection boundary layer flow on a solid sphere subject to a constant surface heat flux boundary condition are considered numerically. Two types of nanoparticles namely graphene and silver suspended in two different types of fluids such as water and kerosene oil. The governing boundary layer equations and the boundary conditions are transformed into nonlinear partial differential equations system and solved numerically, via an implicit finite difference scheme namely Keller box method. The effects on the local wall temperature, the local skin friction coefficient, temperature, velocity and angular velocity are debated for several values of the parameters, namely the nanoparticle volume fraction, the micro-rotation parameter and the mixed convection parameter, by regarding the thermo-physical properties for the nanoparticles and base fluids. Furthermore, numerical results for the local heat transfer and the local skin friction coefficient are obtained, it is found that Ag/GO water has higher in local wall temperature compared with Ag/GO kerosene oil. The accuracy of the results of the local wall temperature and the local skin friction with the published results on Newtonian literature are obtained good agreement.

1. Introduction

Fluid is a material that constantly disfigures with many applications of shear stress (tangential force per unit area). Convectional heat transfer fluids as water, minerals oil and ethylene glycol present a leading role in different modern industrial sections, such as power generation, chemical production, air-conditioning, transportation, and microelectronics. Although many techniques have been applied to modify their heat transfer, their execution is still limited by their low thermal

[*] *Corresponding author.*
E-mail address: abidhussanan@tdtu.edu.vn (Abid Hussanan)

conductivities which prevent performance rising and insufficient heat exchangers. In modern technology, the industrial processes need to improve new types of fluids which are increasingly effective in terms of heat transfer enhancements. In order to conduct this, it has been recently suggesting to insert small amounts of nanometer-volume smaller than 100 nm nanoparticles in base fluids, which is known as well as nanofluids [1]. Moreover, many substances of nanoparticles give of chemically stable, that get from metals, nonmetals, oxides ceramics, carbides, nitrides, layered. The base fluid is usually used as a conductive fluid, like water, oil, polymer solutions, bio-fluids and some known fluids, such as paraffin. Many studies have shown that nanofluids have enhanced thermo-physical characteristics as thermal conductivity, thermal diffusivity, viscosity, and convective heat transfer coefficients compared to these of base fluid [2-5]. Buongiorno [6] published the paper on the convective transport in nanofluids. Tiwari *et al*., [7] considered The nanofluid flow numerically inside a two-sided lid-driven differentially heated square cavity. The nanofluids used to gain perfect thermal advantages at the lowest volume fraction of nanoparticles in the base fluid by Godson *et al*., [8]. Kandelousi [9] as well studied the nanofluid flow and heat transfer through a permeable channel. Haq *et al*., [10] studied the slip effect on heat transfer nanofluid flow past a stretching surface. Several references have on nanofluid as in the universal book by Das *et al*., [11] and more investigations that have been considered to increase the heat-transfer qualities technique by nanofluids, also by those by [5][12-17].

The classical Navier-Stokes model was not suitable to describe Non-Newtonian transport phenomena emerge in many sections of chemical and materials processing engineering. Such fluids show shear, stress and strain relationships which splay significantly. Most non-Newtonian models contain some form of adjustments to the momentum conservation equations. To solve these problemes, Eringen conduced the micropolar material model for microstructural fluids [18]. Moreover, many researchers have studied the micropolar fluid to derive the various results regarding flow problems. Hassanien *et al.,* [19] presented the boundary layer flow and heat transfer from a stretching sheet to a micropolar fluid. Papautsky *et al*., [20] investigated the laminar fluid behaviour in microchannels using micropolar fluid theory. Nazar *et al*., [21] considered stagnation point flow of a micropolar fluid towards a stretching sheet. Exact solutions are obtained by the Laplace transform technique for the unsteady flow of a micropolar fluid by Sherief *et al.,* [22]. Hussanan *et al.,* [23] described the microrotation, temperature, velocity and concentration are considered. The natural convection flow in micropolar fluid over a vertical plate with the Newtonian heating condition and over a solid sphere with convective boundary conditions were considered by Hussanan *et al.,* [24] and Alkasasbeh *et al.,* [25], respectively. Alkasasbeh [26] explores the heat transfer magnetohydrodynamic flow of micropolar Casson fluid on a horizontal circular cylinder with thermal radiation. Free convection on micropolar nanofluid on a solid sphere considered by Swalmeh *et al*., [27] and micropolar forced convection flow on moving surface with magnetic field was studied by Waqas *et al.,* [28].

The heat transfer about boundary layer in the mixed convection flow and a solid sphere has much application in technology, as solving the cooling processes problems. The heat transfer between spheres and airflow experimentally was inspected by Yuge [29]. Recently, the different papers in mixed convection boundary-layer flow over an isothermal solid sphere with several types of fluids were displayed by [30-36].

This article aims to discuss the mixed convection boundary layer flow over a solid sphere in a micropolar nanofluid subject to the boundary condition as constant surface heat flux. Silver (Ag) and graphene oxide (GO) in two based fluids (water and kerosene oil) have been studied in the present consideration. The partial differential equations are obtained from boundary layer equations and solved numerically via efficient implicit finite-difference scheme known as the Keller-box method, as shown by Cebeci *et al.*, [37]. The results of the influence for the nanoparticle volume fraction parameter, the mixed convection parameter and micro-rotation parameter on the local wall temperature, local skin friction, temperature, velocity and angular velocity on a solid sphere are debated and explained in the tables and figures. Also, for the comparison purposes and to check the precision, we have noted the values of the local wall temperature coefficient for the regular Newtonian fluid of this study compared with Nazar *et al.,* [36] at various values of mixed convection parameter in an ideal agreement with $K = 0$ and $\chi = 0$ displayed in Table 1.

2. Problem Formulation

The steady mixed convection boundary-layer flow, in the micropolar nanofluid, with undisturbed free-stream velocity and constant temperature, over a solid sphere of radius a, and two types of nanoparticles such as silver (Ag) and graphene oxide (GO) are suspended in two different types of base fluids such as water and kerosene oil, were considered in this study. Figure 1 displays the physical model and coordinate system that show The convective forced flow to be moving upward. And at the same time the gravity vector *g* acts downward in the opposite direction, while $\bar{x}-$ coordinate is measured along the surface of the solid sphere from the lower stagnation point, $\bar{y}-$ coordinate is measured perpendicular to the surface of the solid sphere. It is also suggeted that the surface of the sphere is preserved at a constant temperature, T_W with $T_W > T_\infty$ for a heated sphere (assisting flow) and $T_W < T_\infty$ for a cooled sphere (opposing flow). The basic steady dimensional continuity, momentum and energy equations for model of micropolar nanofluid, which are supposed by Tiwari and Das [7].

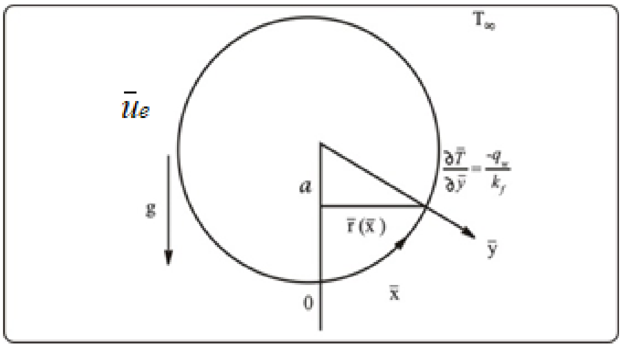

Fig. 1. Physical model and coordinate system

$$\frac{\partial}{\partial \bar{x}}(\bar{r}\,\bar{u}) + \frac{\partial}{\partial \bar{y}}(\bar{r}\,\bar{v}) = 0, \tag{1}$$

$$\bar{u}\frac{\partial \bar{u}}{\partial \bar{x}} + \bar{v}\frac{\partial \bar{u}}{\partial \bar{y}} = \bar{u}_e \frac{d\bar{u}_e}{d\bar{x}} + \left(\frac{\mu_{nf}+\kappa}{\rho_{nf}}\right)\frac{\partial^2 \bar{u}}{\partial \bar{y}^2} + \frac{\left(\chi\rho_s\beta_s + (1-\chi)\rho_f\beta_f\right)}{\rho_{nf}} g\left(T - T_\infty\right)\sin\left(\frac{\bar{x}}{a}\right) + \frac{\kappa}{\rho_{nf}}\frac{\partial \bar{H}}{\partial \bar{y}}, \tag{2}$$

$$\rho_{nf} J\left(\bar{u}\frac{\partial \bar{H}}{\partial \bar{x}} + \bar{v}\frac{\partial \bar{H}}{\partial \bar{y}}\right) = -\kappa\left(2\bar{H} + \frac{\partial \bar{u}}{\partial \bar{y}}\right) + \phi_{nf}\frac{\partial^2 \bar{H}}{\partial \bar{y}^2}, \tag{3}$$

$$\bar{u}\frac{\partial T}{\partial \bar{x}}+\bar{v}\frac{\partial T}{\partial \bar{y}}=\alpha_{nf}\frac{\partial^2 T}{\partial \bar{y}^2}. \tag{4}$$

Subject the boundary conditions

$$\bar{u}=\bar{v}=0,\ \frac{\partial T}{\partial \bar{y}}=\frac{-q_w}{k_{nf}}\ ,\ \bar{H}=-\frac{1}{2}\frac{\partial \bar{u}}{\partial \bar{y}}\ \text{ at }\ \bar{y}=0,$$
$$\bar{u}\to \bar{u}_e(\bar{x}),\ T\to T_\infty\ \ \bar{H}\to 0\ \text{ as }\ \bar{y}\to\infty, \tag{5}$$

we consider that $\bar{r}(\bar{x})=a\sin(\bar{x}/a)$ and $\bar{u}_e(\bar{x})=\frac{3}{2}U_\infty\sin\left(\frac{\bar{x}}{a}\right)$, here $\bar{u}$ and $\bar{v}$ are the velocity components along the $\bar{x}$ - $\bar{y}$ plane, respectively. All other symbols and quantities are shown in nomenclature. Further, $\bar{u}_e(\bar{x})$ is the local free-stream velocity, $\bar{r}(\bar{x})$ is the radial distance from the symmetrical axis to the surface of the sphere, ρ_{nf} is the density of nanofluid, μ_{nf} is the viscosity of nanofluid, α_{nf} is the thermal diffusivity of nanofluid, ϕ_{nf} is the spin gradient viscosity of nanofluid, $\left(\rho C_p\right)_{nf}$ is the heat capacity of nanofluid, and $J=av_f/U_\infty$ is micro-inertia density, which are given by [27]

$$\rho_{nf}=(1-\chi)\rho_f+\chi\rho_f,\ \mu_{nf}=\frac{\mu_f}{(1-\chi)^{2.5}},\ \alpha_{nf}=\frac{k_{nf}}{(\rho C_p)_{nf}},$$
$$(\rho C_p)_{nf}=(1-\chi)(\rho C_p)_f+\chi(\rho C_p)_s,\ \phi_{nf}=\left(\mu_{nf}+\kappa/2\right)j,$$
$$\frac{k_{nf}}{k_f}=\frac{(k_s+2k_f)-2\chi(k_f-k_s)}{(k_s+2k_f)+\chi(k_f-k_s)}. \tag{6}$$

We introduce now the following non-dimensional variables

$$x=\frac{\bar{x}}{a},\ \ y=\mathrm{Re}^{2/5}\left(\frac{\bar{y}}{a}\right),\ r(x)=\frac{\bar{r}(\bar{x})}{a},\ \theta=\mathrm{Re}^{2/5}\left(\frac{T-T_\infty}{aq_w/k}\right),$$
$$u=\frac{\bar{u}}{U_\infty},\ \ v=\mathrm{Re}^{2/5}\left(\frac{\bar{v}}{U_\infty}\right),\ u_e=\frac{\bar{u}_e(\bar{x})}{U_\infty},\ \ H=\left(\frac{a}{U_\infty}\right)\mathrm{Re}^{-2/5}\,\bar{H}, \tag{7}$$

where $\mathrm{Re}=U_\infty a/v_f$ is the Reynolds number and v_f is the kinematic viscosity of the fluid. Substituting the previous variables into Eq. (1)–(4), we obtain the following boundary-layer equations for the problem under dimensionless form.

$$\frac{\partial}{\partial x}\left(ru\right)+\frac{\partial}{\partial y}\left(rv\right)=0, \tag{8}$$

$$
\begin{aligned}
&u\frac{\partial u}{\partial x}+v\frac{\partial u}{\partial y}=u_e\frac{\partial u_e}{\partial x}+\frac{\rho_f}{\rho_{nf}}\left(D(\chi)+K\right)\frac{\partial^2 u}{\partial y^2}\\
&+\frac{1}{\rho_{nf}}\left(\chi\rho_s\left(\frac{\beta_s}{\beta_f}\right)+(1-\chi)\rho_f\right)\lambda\theta\sin x+\frac{\rho_f}{\rho_{nf}}K\frac{\partial H}{\partial y},
\end{aligned}
\tag{9}
$$

$$
u\frac{\partial \theta}{\partial x}+v\frac{\partial \theta}{\partial y}=\frac{1}{\Pr}\left[\frac{k_{nf}/k_f}{(1-\chi)+\chi\left(\rho c_p\right)_s/\left(\rho c_p\right)_f}\right]\frac{\partial^2\theta}{\partial y^2},
\tag{10}
$$

$$
u\frac{\partial H}{\partial x}+v\frac{\partial H}{\partial y}=-\frac{\rho_f}{\rho_{nf}}K\left(2\bar{H}+\frac{\partial \bar{u}}{\partial \bar{y}}\right)+\frac{\rho_f}{\rho_{nf}}\left(D(\chi)+\frac{K}{2}\right)\frac{\partial^2 H}{\partial y^2},
\tag{11}
$$

where $D(\chi)=1/(1-\chi)^{2.5}$, $K=\kappa/\mu_f$ is the micropolar parameter and $\Pr=v_f/\alpha_f$ is the Prandtl number [38, 39]. The mixed convection parameter λ, which is defined as $\lambda=Gr/\mathrm{Re}^2$ with $Gr=g\beta_f\left(aq_w/k\right)\left(a^3/v_f^2\right)$ is the Grashof number for constant surface heat flux boundary conditions. It is important mentioning that $\lambda>0$ for an assisting flow ($T_w>T_\infty$) (heated flow), $\lambda<0$ for an opposing flow $(T_w<T_\infty)$ (cooled flow) and $\lambda=0$ the forced convection flow. The boundary conditions (5) become

$$
\begin{aligned}
&u=v=0,\ \frac{\partial\theta}{\partial y}=-1,\ H=-\frac{1}{2}\frac{\partial u}{\partial y}\ \text{at}\ y=0,\\
&u\to u_e(x)=\frac{3}{2}\sin x,\ \theta\to 0,\ H\to 0\ \text{as}\ y\to\infty,
\end{aligned}
\tag{12}
$$

we assume the following variables to solve Eq. (8)–(11), subject to boundary conditions (12)

$$
\psi=xr(x)f(x.y),\ \theta=\theta(x,y),\ H=xh(x,y),
\tag{13}
$$

where ψ is the stream function defined as

$$
u=\frac{1}{r}\frac{\partial\psi}{\partial y}\ \text{and}\ v=-\frac{1}{r}\frac{\partial\psi}{\partial x},
$$

which satisfies the continuity Eq. (8). Substituting the Eq. (13) into (9) to (11), we obtain the following transformed equations.

$$
\begin{aligned}
&\frac{\rho_f}{\rho_{nf}}(D(\chi)+K)\frac{\partial^3 f}{\partial y^3}+(1+x\cot x)f\frac{\partial^2 f}{\partial y^2}-\left(\frac{\partial f}{\partial y}\right)^2+\frac{1}{\rho_{nf}}\left(\chi\rho_s\left(\frac{\beta_s}{\beta_f}\right)+(1-\chi)\rho_f\right)\lambda\frac{\sin x}{x}\theta\\
&+\frac{9}{4}\frac{\sin x\cos x}{x}+\frac{\rho_f}{\rho_{nf}}K\frac{\partial h}{\partial y}=x\left(\frac{\partial f}{\partial y}\frac{\partial^2 f}{\partial x\partial y}-\frac{\partial f}{\partial x}\frac{\partial^2 f}{\partial y^2}\right),
\end{aligned}
\tag{14}
$$

$$\frac{1}{\Pr}\left[\frac{k_{nf}/k_f}{(1-\chi)+\chi(\rho c_p)_s/(\rho c_p)_f}\right]\frac{\partial^2\theta}{\partial y^2}+f\frac{\partial\theta}{\partial y}(1+x\cot x)=x\left(\frac{\partial f}{\partial y}\frac{\partial\theta}{\partial x}-\frac{\partial f}{\partial x}\frac{\partial\theta}{\partial y}\right), \tag{15}$$

$$\frac{\rho_f}{\rho_{nf}}\left(D(\chi)+\frac{K}{2}\right)\frac{\partial^2 h}{\partial y^2}+(1+x\cot x)f\frac{\partial h}{\partial y}-\frac{\partial f}{\partial y}h-\frac{\rho_f}{\rho_{nf}}K\left(2h+\frac{\partial^2 f}{\partial y^2}\right)=x\left(\frac{\partial f}{\partial y}\frac{\partial h}{\partial x}-\frac{\partial f}{\partial x}\frac{\partial h}{\partial y}\right). \tag{16}$$

The boundary conditions (12) become

$$f=\frac{\partial f}{\partial y}=0,\ \theta'=-1\ ,\ h=-\frac{1}{2}\frac{\partial^2 f}{\partial y^2}\ \text{at}\ y=0,$$
$$\frac{\partial f}{\partial y}\to\frac{3}{2}\sin x\quad \theta\to 0\ h\to 0\ \text{as}\ y\to\infty, \tag{17}$$

we observe that at the lower stagnation point of the sphere, $x\approx 0$ Eq. (14)-(17) reduce to the following differential equations.

$$\frac{\rho_f}{\rho_{nf}}\left(D(\chi)+K\right)f'''+2ff''-(f')^2+\frac{1}{\rho_{nf}}\left(\chi\rho_s\left(\frac{\beta_s}{\beta_f}\right)+(1-\chi)\rho_f\right)\lambda\theta+\frac{\rho_f}{\rho_{nf}}K\frac{\partial h}{\partial y}+\frac{9}{4}=0, \tag{18}$$

$$\frac{1}{\Pr}\left[\frac{k_{nf}/k_f}{(1-\chi)+\chi\left(\rho c_p\right)_s/\left(\rho c_p\right)_f}\right]\theta''+2f\theta'=0, \tag{19}$$

$$\frac{\rho_f}{\rho_{nf}}\left(D(\chi)+\frac{K}{2}\right)h''+2f\,h'-f'h-\frac{\rho_f}{\rho_{nf}}K\left(2h+f''\right)=0. \tag{20}$$

along with the boundary conditions

$$f(0)=f'(0)=0,\ \theta'(0)=-1,\ h(0)=-\frac{1}{2}f''(0)\ \text{as}\ y=0,$$
$$f'\to\frac{3}{2},\ \theta\to 0,\ h\to 0\ \text{as}\ y\to\infty, \tag{21}$$

where the primes denote differentiation with respect to y. The physical quantities of interest are the local skin friction coefficient C_f and and wall temperature θ_W and they can be written as

$$C_f=\left(D(\chi)+\frac{K}{2}\right)x\frac{\partial^2 f}{\partial y^2}(x,0),\ \ \theta(x,0)=\theta_W. \tag{22}$$

3. Numerical Solution

The system of Eq. (14)–(16) subject to boundary conditions (17) are solved numerically via the Keller-box method that presents to be implicit finite difference method, and this method is potent and has a flexible process for parabolic boundary layer flows [37]. The procedures of keller box method have four steps to obtain the solutions of partial differential equations: firstly, write the governing system of equations in the form of a first order system, and then, use centered differences and averages at the midpoint of net rectangles to get finite difference equations, after that, linearize the resulting algebraic equations by Newton's method, finally, write them in a matrix-vector form, and Solve the linear system by the block tridiagonal elimination technique. The accurate numerical results of the linear system were provided and plotted by Matlab® (Version 7).

4. Results and Discussions

The Eq. (14)-(16) subject to the boundary conditions (17) have been solved numerically via the Keller-box method, along with Newton's linearization technique as defined by [37] for various values of parameters, such as the mixed convection parameter λ, the micro-rotation parameter *K*, and the nanoparticle volume fraction χ on the local wall temperature, skin friction coefficient, temperature, velocity and angular velocity fields, at some streamwise positions *x*. For two flow cases as the assisting ($\lambda > 0$) and opposing ($\lambda < 0$). The numerical solution begins at the lower stagnation point of the sphere, $x \approx 0$ with initial profiles as presented by the Eq. (18) to (21), and perform round of the surface of solid sphere up to the separation point. The present results are gained up to $x = 120^o$ only. We have used data related to thermophysical properties of the fluid and nanoparticles as given in Table 1. To accept the accuracy of the present method, we have noted the values of the local wall temperature and local skin friction compared with [35] for the regular Newtonian fluid at various values are in a excellent agreement with *K*=0 and displayed in Table 2.

Table 1
Thermo-physical properties of based fluids and nanoparticles

Physical properties	Water	Kerosene oil	Ag	GO
ρ (kg/m^3)	997.1	783	10500	1800
C_p (J/kg – K)	4179	2090	235	717
K (W/m – K)	0.613	0.145	429	5000
$\beta \times 10^{-5} (K^{-1})$	21	99	1.89	28.4
Pr	6.2	21	…..	…..

Figure 2-5 explain the common correlation between the results of Ag and GO nanoparticles based in water and kerosene oil for the local wall temperature θ_W and the local skin friction C_f respectively, with various values of the nanoparticle volume fraction χ and the micro-rotation parameter *K*, with different values of *x*. We notice that the local wall temperature θ_W in Figure 2 and 4 increase as increases the nanoparticle volume fraction χ and the micro-rotation parameter *K*. Moreover, in Figure 3 and 5 the local skin friction C_f increase with increases χ and *K*, as increase the position *x.* It is also found that in Figure 2-5, the local wall temperature and the local skin friction of Ag/GO water is higher than the Ag/GO kerosene oil, this is because of the density property of water greater than kerosene oil. It is also obtained that GO has the low local wall temperature θ_W as compared to

Ag, and GO has higher in local skin friction C_f compared with Ag. that is because GO has a high thermal conductivity and high density for Ag.

Table 2

Values of local wall temperature θ_W for and $\chi = 0$ (Newtonian fluid), $\Pr = 0.7$ and various values of λ (results in parentheses are those of [36]

χ	λ								
	-2.5	-2	-1.5	-1	-0.5	0.0	0.29	0.30	1.0
0°	1.4890	1.3894	1.3301	1.2877	1.2544	1.2270	1.2131	1.2126	1.1834
	(1.4847)	(1.3863)	(1.3277)	(1.2856)	(1.2525)	(1.2252)	(1.2114)	(1.2109)	(1.1818)
10°	1.5107	1.3990	1.3374	1.2938	1.2599	1.2319	1.2178	1.2173	1.1876
	(1.5027)	(1.3965)	(1.3355)	(1.2921)	(1.2583)	(1.2305)	(1.2164)	(1.2159)	(1.1863)
20°	1.5764	1.4292	1.3597	1.3122	1.2762	1.2466	1.2316	1.2311	1.1996
	(1.5658)	(1.4271)	(1.3583)	(1.3111)	(1.2750)	(1.2455)	(1.2306)	(1.2301)	(1.1991)
30°		1.4871	1.3995	1.3443	1.3042	1.2716	1.2553	1.2539	1.2212
		(1.4855)	(1.3989)	(1.3440)	(1.3035)	(1.2711)	(1.2548)	(1.2542)	(1.2207)
40°		1.5997	1.4630	1.3929	1.3458	1.3082	1.2897	1.2891	1.2516
		(1.5985)	(1.4635)	(1.3938)	(1.3457)	(1.3083)	(1.2898)	(1.2892)	(1.2517)
50°			1.5665	1.4639	1.4043	1.3584	1.3366	1.3359	1.2926
			(1.5691)	(1.4664)	(1.4048)	(1.3594)	(1.3374)	(1.3367)	(1.2932)
60°			1.8361	1.5701	1.4851	1.4256	1.3984	1.3975	1.3437
			(1.8404)	(1.5757)	(1.4865)	(1.4275)	(1.4001)	(1.3993)	(1.3469)
70°				1.7700	1.6000	1.5148	1.4790	1.4778	1.4103
				(1.7728)	(1.6028)	(1.5181)	(1.4818)	(1.4807)	(1.4147)
80°					1.7743	1.6358	1.5843	1.5828	1.4937
					(1.7869)	(1.6410)	(1.5887)	(1.5871)	(1.4997)
90°						1.8096	1.7254	1.7184	1.5979
						(1.8181)	(1.7319)	(1.7295)	(1.6058)
100°						2.0978	1.9247	1.9205	1.7283
						(2.1286)	(1.9347)	(1.9303)	(1.7384)
110°							2.2131	2.2397	1.8921
							(2.2688)	(2.2572)	(1.9050)
120°								5.0907	2.0992
								(5.1090)	(2.1152)

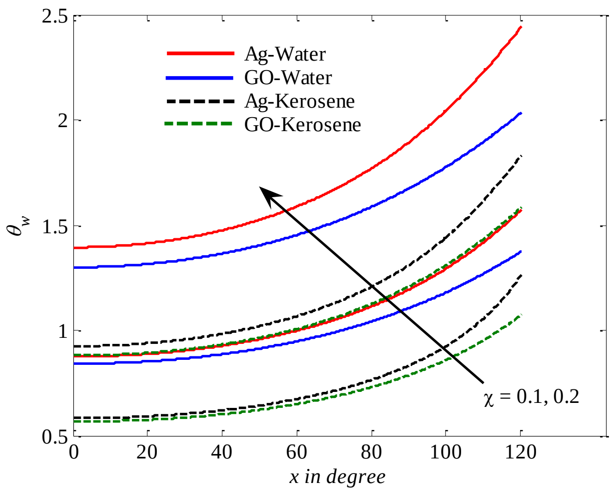

Fig. 2. Comparison of the local wall temperature using Ag/GO in water and kerosene oil-based

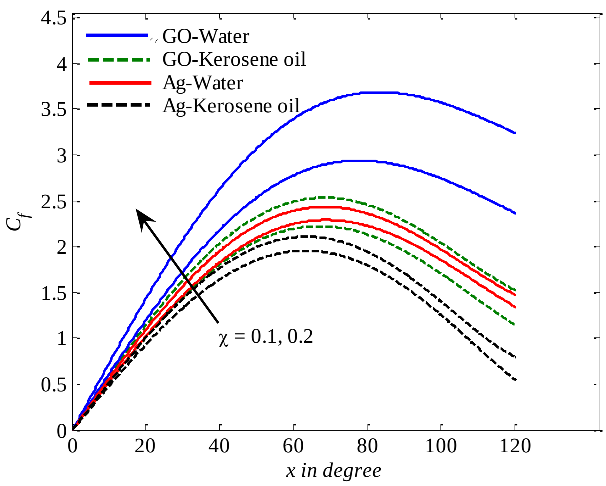

Fig. 3. Comparison of the local skin friction using Ag/GO in water and kerosene oil-based

nanofluids, for various values of *x* and χ when $\lambda = 5$ and $K = 0.2$.

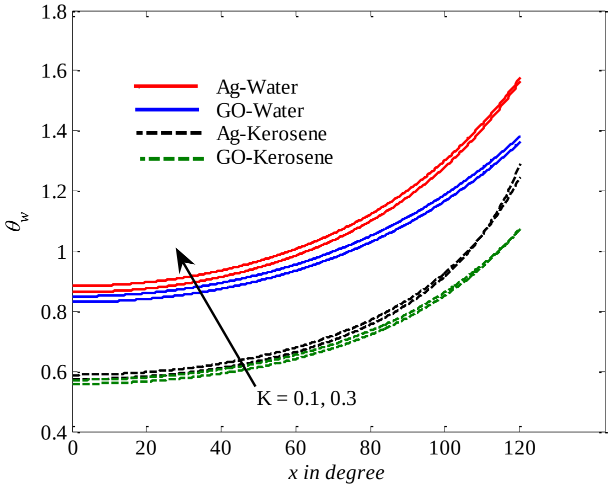

Fig. 4. Comparison of the local wall temperature using Ag/GO in water and kerosene oil-based nanofluids, for various values of *x* and *K* when $\lambda = 5$ and $\chi = 0.1$.

nanofluids, for various values of *x* and χ, when $\lambda = 5$ and $K = 0.2$.

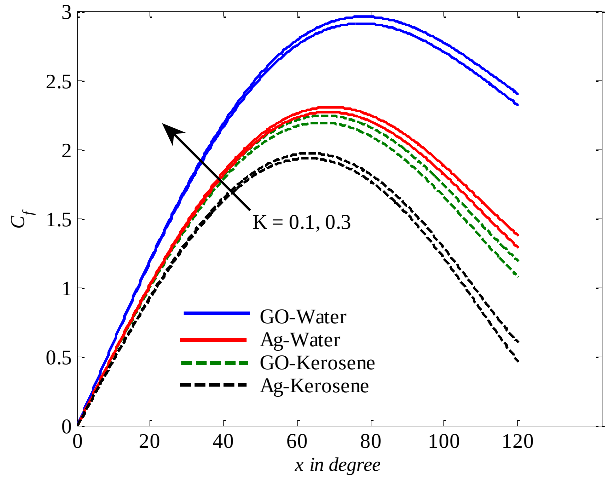

Fig. 5. Comparison of the local skin friction using Ag/GO in water and kerosene oil-based nanofluids, for various values of *x* and *K*, when $\lambda = 5$ and $\chi = 0.1$.

The effect of the mixed convection parameter λ on local wall temperature θ_W and the local skin friction C_f are shown in Figure 6-7. It is shown that the local wall temperature θ_W decrease as increase the values of, but when the mixed convection parameter λ increase, the local skin friction C_f increase. Furthermore, the Ag/GO water has a higher value of the local wall temperature and the local skin friction compared to Ag/GO kerosene oil, except when ($\lambda < 0$) (cooled sphere), the local skin friction C_f of Ag/GO kerosene oil is higher than water, since to physical properties of water and kerosene oil. Besides that, Ag has a higher local wall temperature θ_W and local skin friction C_f as compared to GO, for several values of λ except when ($\lambda > 0$) (heated sphere), the local skin friction of GO has lower than Ag.

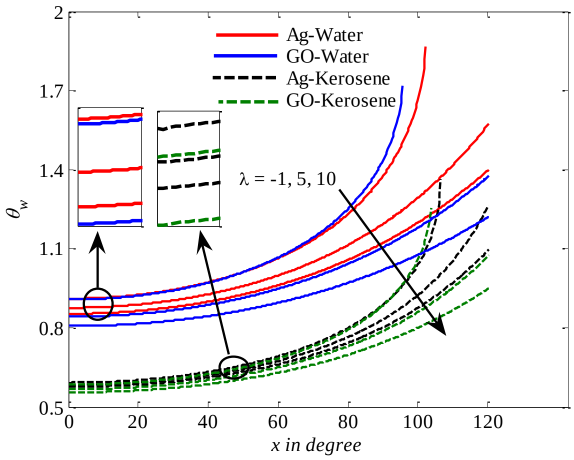

Fig. 6. Comparison of the local wall temperature using Ag/GO in water and kerosene oil-based

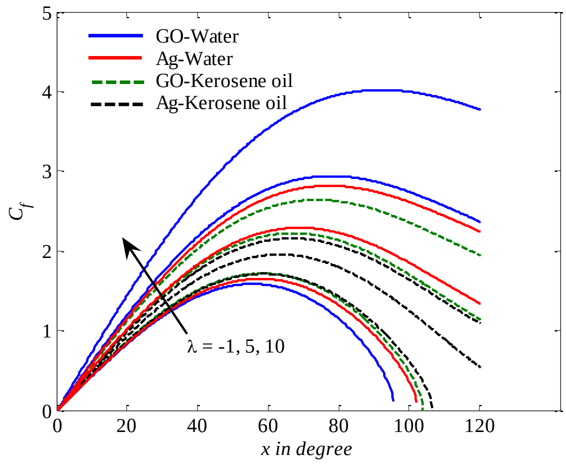

Fig. 7. Comparison of the local skin friction using Ag/GO in water and kerosene oil-based

nanofluids, for various values of *x* and λ, when $K = 0.2.$ and $\chi = 0.2.$

nanofluids, for various values of *x* and λ, when $K = 0.2.$ and $\chi = 0.2.$

Figure 8 to 13 illustrate the influence of the nanoparticle volume fraction χ and the micro-rotation parameter *k* on the temperature profiles, the velocity profiles, and the angular velocity respectively, of GO in water and kerosene oil at the lower stagnation point of a solid sphere, $x \approx 0$. It can be seen that when the nanoparticle volume fraction χ and the micro-rotation parameter *k* increase, the velocity profiles and the angular velocity profiles decrease, while the temperature profiles increase. Besides that, it is also found that GO water has a higher temperature, velocity and angular velocity compared with GO kerosene oil for every value of the nanoparticle volume fraction χ and the micro-rotation parameter *K*.

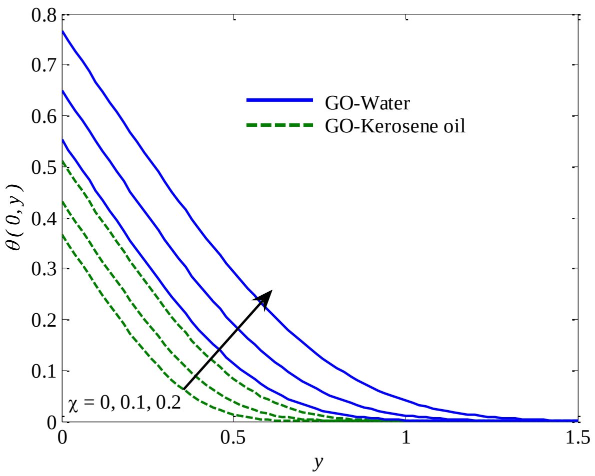

Fig. 8. Temperature profiles at $x \approx 0$ using GO in water and kerosene oil-based nanofluids, for various values of χ, when $\lambda = 3$ and $K = 0.3$

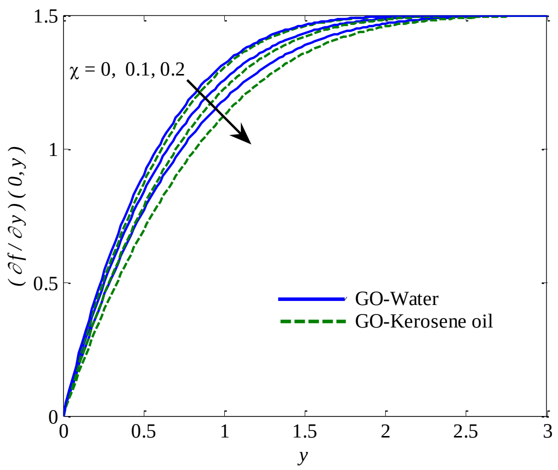

Fig. 9. Velocity profiles at $x \approx 0$ using GO in water and kerosene oil-based nanofluids, for various values of χ, when $\lambda = 3$ and $K = 0.3$

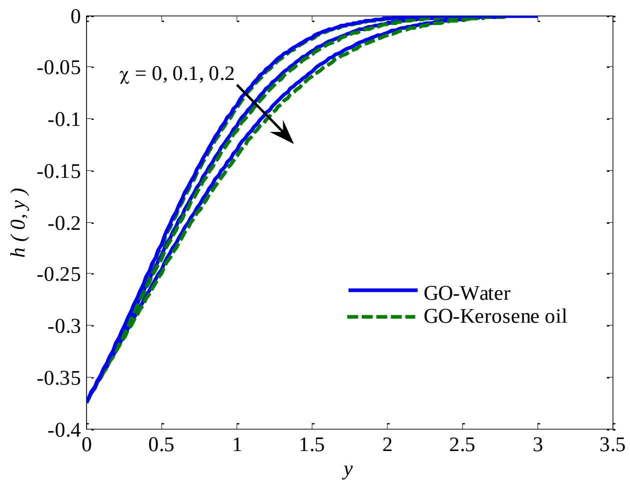

Fig. 10. Angular velocity profiles at $x \approx 0$ using GO in water and kerosene oil-based nanofluids, for various values of χ, when $\lambda = 3$ and $K = 0.3$

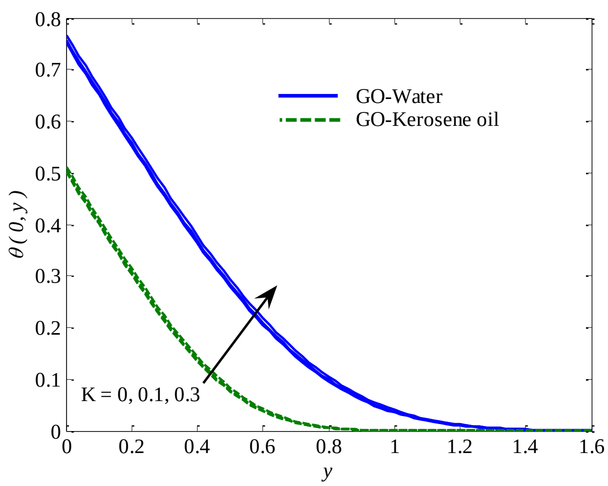

Fig. 11. Temperature profiles at $x \approx 0$ using GO in water and kerosene oil-based nanofluids, for various values of *K*, when $\lambda = 3$ and $\chi = 0.2$

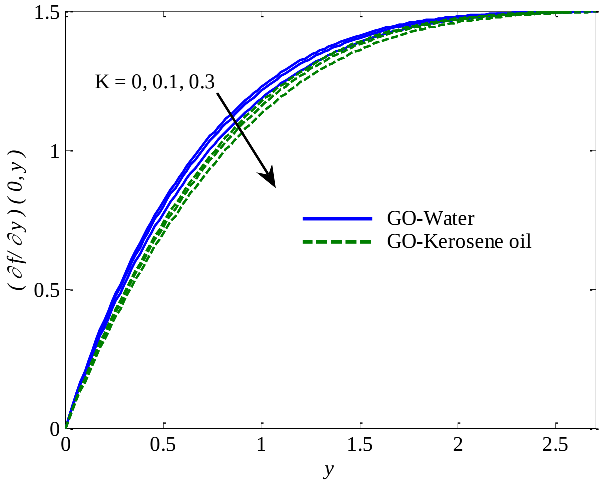

Fig. 12. velocity profiles at $x \approx 0$ using GO in water and kerosene oil-based nanofluids, for various values of *K*, when $\lambda = 3$ and $\chi = 0.2$

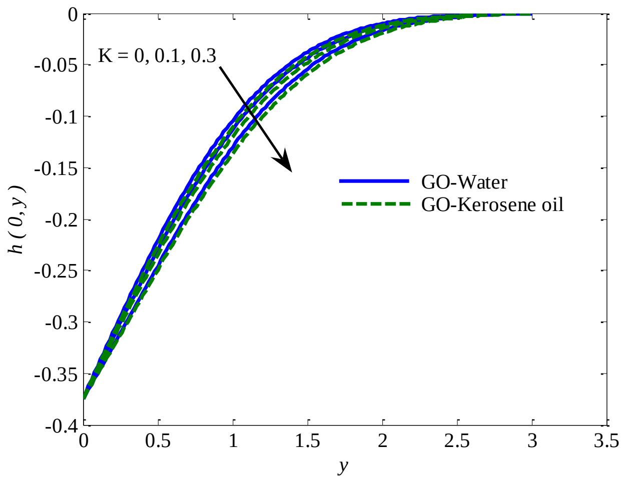

Fig. 13. Angular velocity profiles at $x \approx 0$ using GO in water and kerosene oil-based nanofluids, for various values of *K*, when $\lambda = 3$ and $\chi = 0.2$

Figure 14-16 explain the effects of the mixed convection parameter λ on temperature, velocity and angular velocity profiles of GO in water and kerosene oil respectively. It is found that as the mixed convection parameter λ increase, the values of the temperature decrease, and the velocity and the angular increase. Moreover, Figure 14 obvious that GO water has high of a temperature as compared to GO kerosene oil with increasing the values of the mixed convection parameter λ. From Figure 15 and 16 that ($\lambda > 0$) (heated sphere) the GO water has high of a velocity and angular velocity as compared to GO kerosene oil, but the opposite happens when ($\lambda < 0$). (cooled sphere), the GO water has a lower velocity and the angular velocity than GO kerosene oil.

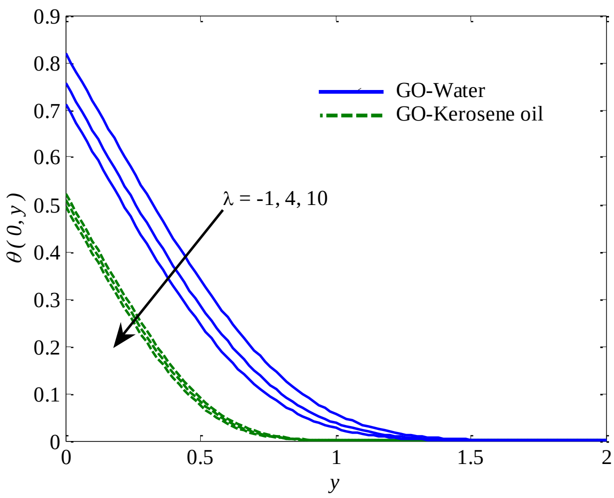

Fig. 14. Temperature profiles at $x \approx 0$ using GO in water and kerosene oil-based nanofluids, for various values of λ, when $K = 0.3.$ and $\chi = 0.2$

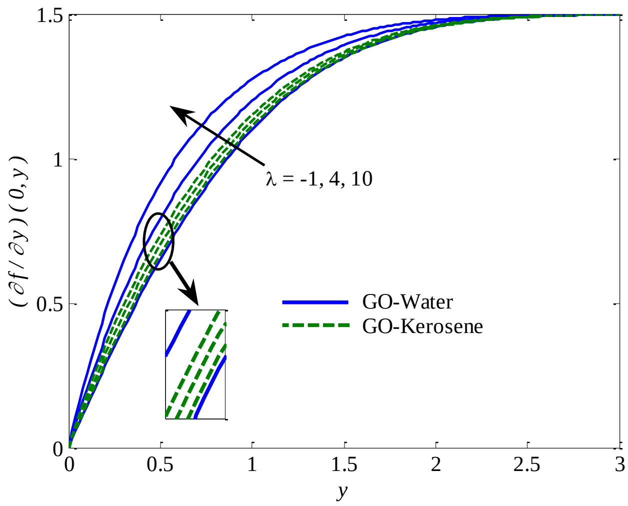

Fig. 15. Velocity profiles at $x \approx 0$ using GO in water and kerosene oil-based nanofluids, for various values of λ, when $K = 0.3.$ and $\chi = 0.2$

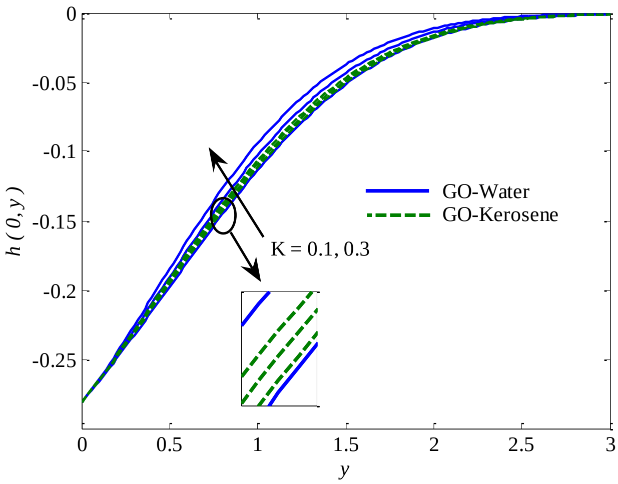

Fig. 16. Angular velocity profiles at $x \approx 0$ using GO in water and kerosene oil-based nanofluids, for various values of λ, when $K = 0.3.$ and $\chi = 0.2$

5. Conclusions

In this paper, we have numerically investigated the mixed convection boundary-layer flow about the solid sphere in a micropolar nanofluid with constant surface heat flux. We discussed into the effects of the mixed convection parameter λ, the nanoparticle volume fraction χ, the micro-rotation parameter *K* and the type of nanoparticles Ag and GO suspended in two based fluids, such as water and kerosene oil, on the flow and heat transfer characteristics. The problem is modelled and then solved via Keller box method. From this study, we could conclude the following conclusions.

i. The Ag/GO water has higher local wall temperature and local skin friction as compared to Ag/GO kerosene oil, except when ($\lambda < 0$) (cooled sphere), the local skin friction of Ag/GO kerosene oil becomes higher than Ag/GO water.
ii. An increase in χ and *K* led to an increase of the local wall temperature, but when the and λ increase, the wall temperature decrease.
iii. The local wall temperature for Ag water/kerosene oil is higher than GO water/kerosene oil for different value of the parameters χ, *K,* and λ.
iv. The GO water has a higher temperature, velocity and angular velocity compared with GO kerosene oil for every value of parameters χ and *K*.
v. The GO water has a higher velocity and angular velocity compared with GO kerosene oil for every value of a parameter λ, but the opposite happens when the case of the cooled sphere ($\lambda < 0$).

Acknowledgement
The corresponding author would like to thanks Ton Duc Thang University, Vietnam for the financial support. This research was funded by a grant from Ministry of Higher Education of Malaysia (FRGS Grant R.J130000.7824.4X172).

References

[1] Choi, Stephen US, and Jeffrey A. Eastman. *Enhancing thermal conductivity of fluids with nanoparticles*. No. ANL/MSD/CP-84938; CONF-951135-29. Argonne National Lab., IL (United States), 1995.

[2] Choi, Stephen US. "Nanofluids: from vision to reality through research." *Journal of Heat transfer* 131, no. 3 (2009): 033106.

[3] Yu, Wenhua, David M. France, Jules L. Routbort, and Stephen US Choi. "Review and comparison of nanofluid thermal conductivity and heat transfer enhancements." *Heat transfer engineering* 29, no. 5 (2008): 432-460.

[4] Tyler, T., O. Shenderova, G. Cunningham, J. Walsh, J. Drobnik, and G. McGuire. "Thermal transport properties of diamond-based nanofluids and nanocomposites." *Diamond and related materials* 15, no. 11-12 (2006): 2078-2081.

[5] Das, Sarit Kumar, Stephen US Choi, and Hrishikesh E. Patel. "Heat transfer in nanofluids—a review." *Heat transfer engineering* 27, no. 10 (2006): 3-19

[6] Buongiorno, Jacopo. "Convective transport in nanofluids." *Journal of heat transfer* 128, no. 3 (2006): 240-250.

[7] Tiwari, Raj Kamal, and Manab Kumar Das. "Heat transfer augmentation in a two-sided lid-driven differentially heated square cavity utilizing nanofluids." *International Journal of Heat and Mass Transfer* 50, no. 9-10 (2007): 2002-2018.

[8] Godson, Lazarus, B. Raja, D. Mohan Lal, and S. Wongwises. "Enhancement of heat transfer using nanofluids—an overview." *Renewable and sustainable energy reviews* 14, no. 2 (2010): 629-641.

[9] Kandelousi, Mohsen Sheikholeslami. "KKL correlation for simulation of nanofluid flow and heat transfer in a permeable channel." *Physics Letters A* 378, no. 45 (2014): 3331-3339.

[10] Haq, Rizwan Ul, Sohail Nadeem, Zafar Hayyat Khan, and N. F. M. Noor. "Convective heat transfer in MHD slip flow over a stretching surface in the presence of carbon nanotubes." *Physica B: condensed matter* 457 (2015): 40-47.

[11] Das, Sarit K., Stephen U. Choi, Wenhua Yu, and T. Pradeep. *Nanofluids: science and technology*. John Wiley & Sons, 2007.

[12] Abu-Nada, Eiyad. "Application of nanofluids for heat transfer enhancement of separated flows encountered in a backward facing step." *International Journal of Heat and Fluid Flow* 29, no. 1 (2008): 242-249.

[13] Oztop, Hakan F., and Eiyad Abu-Nada. "Numerical study of natural convection in partially heated rectangular enclosures filled with nanofluids." *International journal of heat and fluid flow* 29, no. 5 (2008): 1326-1336.

[14] Kandelousi, Mohsen Sheikholeslami. "Effect of spatially variable magnetic field on ferrofluid flow and heat transfer considering constant heat flux boundary condition." *The European Physical Journal Plus* 129, no. 11 (2014): 248.

[15] Qasim, M., Z. H. Khan, R. J. Lopez, and W. A. Khan. "Heat and mass transfer in nanofluid thin film over an unsteady stretching sheet using Buongiorno's model." *The European Physical Journal Plus* 131, no. 1 (2016): 16.

[16] Hussanan, Abid, Ilyas Khan, Hasmawani Hashim, Muhammad Khairul Anuar, Nazila Ishak, Norhafizah Md Sarif, and Mohd Zuki Salleh. "Unsteady MHD flow of some nanofluids past an accelerated vertical plate embedded in a porous medium." *Jurnal Teknologi* 78, no. 2 (2016).

[17] Tlili, I., W. A. Khan, and Ilyas Khan. "Multiple slips effects on MHD SA-Al2O3 and SA-Cu non-Newtonian nanofluids flow over a stretching cylinder in porous medium with radiation and chemical reaction." *Results in physics* 8 (2018): 213-222.

[18] Eringen, A. C. "Theory of micropolar fluids, Journal of Mathematics and Mechanics." (1966): 1-18.

[19] Hassanien, I. A., A. A. Abdullah, and R. S. R. Gorla. "Numerical solutions for heat transfer in a micropolar fluid over a stretching sheet." *Applied Mechanics and Engineering* 3, no. 3 (1998): 377-391.

[20] Papautsky, Ian, John Brazzle, Timothy Ameel, and A. Bruno Frazier. "Laminar fluid behavior in microchannels using micropolar fluid theory." *Sensors and actuators A: Physical* 73, no. 1-2 (1999): 101-108.

[21] Nazar, Roslinda, Norsarahaida Amin, Diana Filip, and Ioan Pop. "Stagnation point flow of a micropolar fluid towards a stretching sheet." *International Journal of Non-Linear Mechanics* 39, no. 7 (2004): 1227-1235.

[22] Sherief, H. H., M. S. Faltas, and E. A. Ashmawy. "Exact solution for the unsteady flow of a semi-infinite micropolar fluid." *Acta Mechanica Sinica* 27, no. 3 (2011): 354-359.

[23] Hussanan, Abid, Mohd Zuki Salleh, Ilyas Khan, and Razman Mat Tahar. "Heat and mass transfer in a micropolar fluid with Newtonian heating: an exact analysis." *Neural Computing and Applications* 29, no. 6 (2018): 59-67.

[24] Hussanan, Abid, Mohd Zuki Salleh, Ilyas Khan, and Razman Mat Tahar. "UNSTEADY FREE CONVECTION FLOW OF A MICROPOLAR FLUID WITH NEWTONIAN HEATING: Closed Form Solution." *Thermal Science* 21, no. 6 (2017).

A. Hussanan, M. Z. Salleh, I. Khan, and R. M. Tahar, "Unsteady free convection flow of a micropolar fluid with Newtonian heating: Closed form solution," *Thermal Science,* (2015) *:* 125-125

[25] Alkasasbeh, Hamzeh Taha, Mohd Zuki Salleh, Razman Mat Tahar, Roslinda Nazar, and Ioan Pop. "Free Convection Boundary Layer Flow on a Solid Sphere with Convective Boundary Conditions in a Micropolar Fluid." *World Applied Sciences Journal* 32, no. 9 (2014): 1942-1951.

[26] Alkasasbeh, Hamzeh. "Numerical Solution on Heat Transfer Magnetohydrodynamic Flow of Micropolar Casson Fluid over a Horizontal Circular Cylinder with Thermal Radiation." *Frontiers in Heat and Mass Transfer (FHMT)* 10 (2018).

[27] Swalmeh, Mohammed Z., Hamzeh T. Alkasasbeh, Abid Hussanan, and Mustafa Mamat. "Heat transfer flow of Cu-water and Al2O3-water micropolar nanofluids about a solid sphere in the presence of natural convection using Keller-box method." *Results in Physics* 9 (2018): 717-724.

[28] Waqas, Hassan, Sajjad Hussain, Humaira Sharif, and Shamila Khalid. "MHD forced convective flow of micropolar fluids past a moving boundary surface with prescribed heat flux and radiation." *Journal of Advances in Mathematics and Computer Science* (2017): 1-14.

[29] Yuge, T. "Experiments on heat transfer from spheres including combined natural and forced convection." *Journal of Heat Transfer* 82, no. 3 (1960): 214-220.

[30] Hieber, C. A., and B. Gebhart. "Mixed convection from a sphere at small Reynolds and Grashof numbers." *Journal of Fluid Mechanics* 38, no. 1 (1969): 137-159.

[31] Chen, T. S., and Aleksandros Mucoglu. "Analysis of mixed forced and free convection about a sphere." *International Journal of Heat and Mass Transfer* 20, no. 8 (1977): 867-875.

[32] Dennis, S. C. R., and J. D. A. Walker. "Calculation of the steady flow past a sphere at low and moderate Reynolds numbers." *Journal of Fluid Mechanics* 48, no. 4 (1971): 771-789.

[33] Tham, L., R. Nazar, and I. Pop. "Mixed convection boundary-layer flow about an isothermal solid sphere in a nanofluid." *Physica Scripta* 84, no. 2 (2011): 025403.

[34] Alkasasbeh, Hamzeh Taha, M. Z. Salleh, R. M. Tahar, R. Nazar, and I. Pop. "Numerical Solution for Mixed Convection Boundary Layer Flow About a Solid Sphere in a Micropolar Fluid with Convective Boundary Conditions." *World Applied Sciences Journal* 33, no. 9 (2015): 1472-1481.

[35] Alkasasbeh, Hamzeh T., Mohammed Z. Swalmeh, Abid Hussanan, and Mustafa Mamat. "Effects of Mixed Convection on Methanol and Kerosene Oil Based Micropolar Nanofluid Containing Oxide Nanoparticles." *CFD Letters* 11, no. 1 (2019): 70-83.

[36] Nazar, Roslinda, Norsarahaida Amin, and Ioan Pop. "Mixed convection boundary layer flow from a sphere with a constant surface heat flux in a micropolar fluid." *Journal of Energy Heat and Mass Transfer* 24, no. 3 (2002): 195-212.

[37] Cebeci, Tuncer, and Peter Bradshaw. *Physical and computational aspects of convective heat transfer*. Springer Science & Business Media, 2012.

[38] Raju, R. Srinivasa, G. Jithender Reddy, J. Anand Rao, and M. M. Rashidi. "Thermal diffusion and diffusion thermo effects on an unsteady heat and mass transfer magnetohydrodynamic natural convection Couette flow using FEM." *Journal of Computational Design and Engineering* 3, no. 4 (2016): 349-362.

[39] Reddy, G. Jitthender, R. Srinivasa Raju, J. Anand Rao, and Rama Subba Reddy Gorla. "Unsteady MHD heat transfer in Couette flow of water at 4° c in a rotating system with ramped temperature via finite element method." *International Journal of Applied Mechanics and Engineering* 22, no. 1 (2017): 145-161.